

Cite this: *Mater. Adv.*, 2023,  
4, 4390

# Colorimetric sensing of calcium carbide over banana peels using 5,5'-dithiobis-(2-nitrobenzoic acid) (DTNB) as a rapid chemoreceptor: a point of care tool for food fraud analysis†

Sonam Sonwal,<sup>a</sup> Shruti Shukla,<sup>\*bc</sup> Munirah Alhammadi,<sup>a</sup> Reddicherla Umaphathi,<sup>ib a</sup>  
Hemanth P. K. Sudhani,<sup>d</sup> Youngjin Cho<sup>\*e</sup> and Yun Suk Huh<sup>ib \*a</sup>

Point-of-care sensing systems have led to the rapid development of smart and portable devices in the field of analyte detection technology. The high flow of artificially ripened fruits (ARFs) in the market results in severe health risks, and simultaneously, the unavailability of consumer-level 1st screening tool flares up its exigency. Calcium carbide (CaC<sub>2</sub>) is a hazardous artificial fruit ripening agent. In this study, a portable one-step colorimetric sensor was developed for the detection of CaC<sub>2</sub> on the surface of ARFs. The presence of CaC<sub>2</sub> was detected using 5,5'-dithiobis-(2-nitrobenzoic acid). The colorimetric reaction of DTNB detected CaC<sub>2</sub> by the free sulfhydryl group detection method which produced a yellow color; the free sulfhydryl group is present as an impurity in CaC<sub>2</sub>. The proposed assay displayed an LOD of 50 ppm with a detection time of a few seconds to 1 minute. It exhibited a rapid, highly sensitive and highly selective response, with a linear dynamic range of 0–4000 ppm and R<sup>2</sup> values of 0.993 and 0.994 for 323 and 412 nm peaks, respectively. The development of this inexpensive, naked eye, portable, and easily accessible CaC<sub>2</sub> sensor reinforces the suggestion that it could bridge the gap between conventional detection techniques and consumer-level detection methods. Our sensor could be useful as a 1st screening tool in various fields, including agriculture, food, and cosmetics industries.

Received 4th May 2023,  
Accepted 21st July 2023

DOI: 10.1039/d3ma00212h

rsc.li/materials-advances

## 1. Introduction

Calcium carbide (CaC<sub>2</sub>) is a gray carcinogenic synthetic compound manufactured to fulfill the rapidly increasing global demand of the developing sectors, such as iron desulfurization (sulfur removal from iron, including cast iron, pig iron, and steel) and artificial ripening of pre-harvested fruits.<sup>1,2</sup> The end uses of CaC<sub>2</sub> in different regions globally are expected to exceed US\$ 31 billion by 2031.<sup>3</sup> Extended application and global

utilization of CaC<sub>2</sub> are strong evidence of its widespread availability in the market at a low or no cost. There is a significant amount of “CaS” (sulfides) present in CaC<sub>2</sub> organically, as well as in the CaC<sub>2</sub> coming from steel industries after the desulfurization process.<sup>4–6</sup> CaC<sub>2</sub> is widely used commercially and at home to accelerate the artificial ripening of fruits and crops.<sup>7,8</sup> India is leading the world in banana, papaya, and mango production. Unfortunately, traders illegally use CaC<sub>2</sub> to artificially ripen these fruits, which violates the Food Safety and Standards Act of 2006 regulations<sup>9,10</sup> under the Food Safety and Standards Authority of India (FSSAI).<sup>11</sup> FSSAI has prohibited the use of CaC<sub>2</sub> due to its serious health risks under the provisions of sub-regulation 2.3.5 of the Food Safety and Standards (Prohibition and Restriction on Sales) Regulations, 2011.<sup>12–15</sup> In the current scenario, rampant fruit adulteration (artificial ripening of fruits) has been seized, and there is massive loss and waste of agricultural food, particularly in India. The FSSAI and the Food and Drug Administration (FDA) in India are on the lookout for cases of artificially ripened mangoes and have uncovered numerous cases of food fraud,<sup>16</sup> including the Guwahati, India case,<sup>17</sup> Ukkadam city, Coimbatore, India case,<sup>18</sup> and Gudivada and Machilipatnam, India case.<sup>19</sup>

CaC<sub>2</sub> produces heat when it comes into contact with moisture, which can cause burns and damage to the mucosa, skin,

<sup>a</sup> NanoBio High-Tech Materials Research Center, Department of Biological Sciences and Bioengineering, Inha University, Incheon 22212, South Korea.  
E-mail: yunsuk.huh@inha.ac.kr

<sup>b</sup> TERI-Deakin Nanobiotechnology Centre, Division of Sustainable Agriculture, The Energy and Resources Institute, India Habitat Centre, Lodhi Road, New Delhi, 11003, India. E-mail: shruti.shukla@teri.res.in

<sup>c</sup> Department of Nanotechnology, North-Eastern Hill University (NEHU), East Khasi Hills, Shillong, Meghalaya, 793022, India. E-mail: shrutishukla1983@gmail.com

<sup>d</sup> Department of Biotechnology, School of Liberal Arts & Sciences, Sree Vidyanikethan Engineering College, Mohan Babu University, Tirupati, 517102, India

<sup>e</sup> Food Safety and Distribution Research Group, Korea Food Research Institute, Wanju 55365, Republic of Korea. E-mail: yjcho74@kfri.re.kr

† Electronic supplementary information (ESI) available. See DOI: <https://doi.org/10.1039/d3ma00212h>





in this study. Inductively coupled plasma-optical emission spectroscopy (ICP-OES) was used for the validation of the fabricated sensor.

## 2.2. DTNB preparation

$\text{Na}_2\text{HPO}_4 \cdot 7\text{H}_2\text{O}$  (10.107 g) and  $\text{NaH}_2\text{PO}_4 \cdot \text{H}_2\text{O}$  (1.697 g) were dissolved in 500 mL of distilled water to prepare a 0.1 M sodium phosphate buffer, and the pH was further adjusted to 7.4, 6, 7, 8, and 9. DTNB solutions of various concentrations (0.5 mM, 1 mM, 10 mM, and 15 mM) were prepared using the 0.1 M sodium phosphate buffer. For optimization, different DTNB concentrations were prepared using different pH values of sodium phosphate buffer.

## 2.3. $\text{CaC}_2$ solution preparation

$\text{CaC}_2$  powder was dissolved in DW, and a 10 000 ppm  $\text{CaC}_2$  stock solution was prepared. Using the stock solution, 0, 10, 50, 100, 150, 200, 250, 500, 750, 1000, 2000, 4000, 6000, and 10 000 ppm solutions were prepared and used for the colorimetric assay.

## 2.4. $\text{CaC}_2$ sensing procedure

$\text{CaC}_2$  solution (from the stock solution) and DTNB solution were mixed to obtain a colorimetric signal for solution-based colorimetric  $\text{CaC}_2$  detection and Ellman's reagent reduction. Four different combinations of  $\text{CaC}_2$  and DTNB solutions were used for this experiment: (a) 15 mM DTNB (pH 9; 150  $\mu\text{L}$ ) and  $\text{CaC}_2$  (850  $\mu\text{L}$ ), (b) 15 mM DTNB (pH 7; 150  $\mu\text{L}$ ) and  $\text{CaC}_2$  (850  $\mu\text{L}$ ), (c) 0.5 mM DTNB (pH 9; 150  $\mu\text{L}$ ) and  $\text{CaC}_2$  (850  $\mu\text{L}$ ), and (d) 0.5 mM DTNB (pH 7; 150  $\mu\text{L}$ ) and  $\text{CaC}_2$  (850  $\mu\text{L}$ ) [Fig. S1, ESI<sup>†</sup>]. Colorimetric sensing was then conducted using the optimized combination (a).

## 2.5. Color signal characterization

Sensor color change was assessed using digital images of the films before and after exposure to the  $\text{CaC}_2$  solution. The images of the enzymatic chemoreceptor-based DTNB sensors were captured using a digital camera. The absorption spectra of all  $\text{CaC}_2$  concentrations were recorded using a UV spectrophotometer. Raw bananas were used as the sample model for real-time detection in this study. Our sensor can be used for a variety of other fruits, including those that are subjected to artificial ripening, such as mango, pear, apple, papaya, grapes, and plum. Raw bananas were artificially ripened by applying (spraying)<sup>51</sup> 10,000 ppm (minimum concentration for ripening)<sup>24</sup>  $\text{CaC}_2$  solution on them and storing them in a closed chamber in the dark at room temperature for two days. After two days, the bananas were taken out and examined for the presence of  $\text{CaC}_2$ .  $\text{CaC}_2$  was detected by swabbing a wet (water) cotton plug over a banana peel and allowing the analyte to absorb into the cotton plug. After swabbing all the exposed areas, the cotton plug was squeezed into a vial containing the DTNB solution for the colorimetric detection of  $\text{CaC}_2$  in a real sample.

## 2.6. XRF, SEM, EDX, and XPS characterization

X-ray fluorescence (XRF) analysis was used to study the entire  $\text{CaC}_2$  composition [Table S1, ESI<sup>†</sup>]. Scanning electron microscopy (SEM)

images of  $\text{CaC}_2$  were captured and analyzed to study its morphology (microstructure ameliorates) [Fig. 1(A)]. SEM mapping and X-ray photoelectron spectroscopy (XPS) analysis were used to examine the distribution of elements at the core level and fitted XPS data for carbon, calcium, and sulfur distribution [Fig. 1(B)–(K)–(1–3)]. Data of XPS analysis for the distribution of remaining elements at the core level are mentioned in Fig. S2 (ESI<sup>†</sup>).

## 2.7. Matrix effect and sulfate test

The banana matrix also contained natural sulfate. We used the proposed sensing technique to cross-check and confirm the selectivity and performance of the developed sensor. An extraction technique was used to prepare the banana matrix sample. By combining 1 g of banana, 3 mL of phosphate buffer, and 5 g of glass beads in a plastic bottle and vigorously shaking it with a vortex, banana pulp was made. For matrix analysis, the pulp extract was separated from the glass beads and combined with the DTNB solution (sulfate test) [Fig. S3, ESI<sup>†</sup>]. Other sulfates (ammonium sulfate, manganese sulfate, magnesium sulfate, potassium sulfate, sodium sulfate, and copper sulfate) were also tested to determine the sensitivity and selectivity of the developed sensor [Fig. S5, ESI<sup>†</sup>].

# 3. Results and discussion

## 3.1. Compositional and structural study of $\text{CaC}_2$

The morphology and chemical composition of commercial  $\text{CaC}_2$  were examined by the HR-SEM and energy-dispersive X-ray (EDX) elemental mapping studies.  $\text{CaC}_2$  is seen to be a large irregular crystal in the SEM image. The surface elemental composition of the crystals was analyzed by elemental mapping studies which evidently showed the presence of calcium (Ca), sulphur (S), silicon (Si), phosphorous (P), magnesium (Mg), aluminum (Al), and iron (Fe) [Fig. 1(A)–(I)]. The trace elements detected like S, Si, P, Mg, Al, Fe, *etc.* are impurities present in the commercial calcium carbide available in the market. XRF data [Table S1, ESI<sup>†</sup>] show the high sulfide content in calcium carbide powder. The molecular states and structure of the compound were elucidated from XPS characterization. In Fig. 1(J)–(1–3), the core level C1s, Ca2p, and S2p spectra of  $\text{CaC}_2$  evidently established the presence of C, Ca, and S, respectively. The fitted peaks of the same are shown in Fig. 1(K)–(1–3). The C1s spectrum exhibits three prominent peaks, respectively, at 284.4 eV which corresponds to the  $\text{sp}^3\text{-C}/\text{sp}^2\text{-C}$  hybridized carbon, at 286.4 eV which corresponds to the  $\text{sp-C}$  carbon, and finally, at 290 eV representing C–O–C bonding.<sup>52,53</sup> The Ca2p core level spectra can be resolved into three components. The peak corresponds to the binding energy 346.3 eV, representing  $\text{Ca}2\text{p}_{3/2}$  and another prominent peak at 350.5 eV corresponds to  $\text{Ca}2\text{p}_{1/2}$ .<sup>54</sup> The presence of  $\text{CaC}_2$  species was further confirmed by the peak at 348 eV S2p core level spectrum which exhibited two prominent peaks at 163.9 eV and 162.5 eV, respectively, representing metallic sulphur and CaS bonding present in the commercial calcium carbide as an impurity.<sup>55</sup>



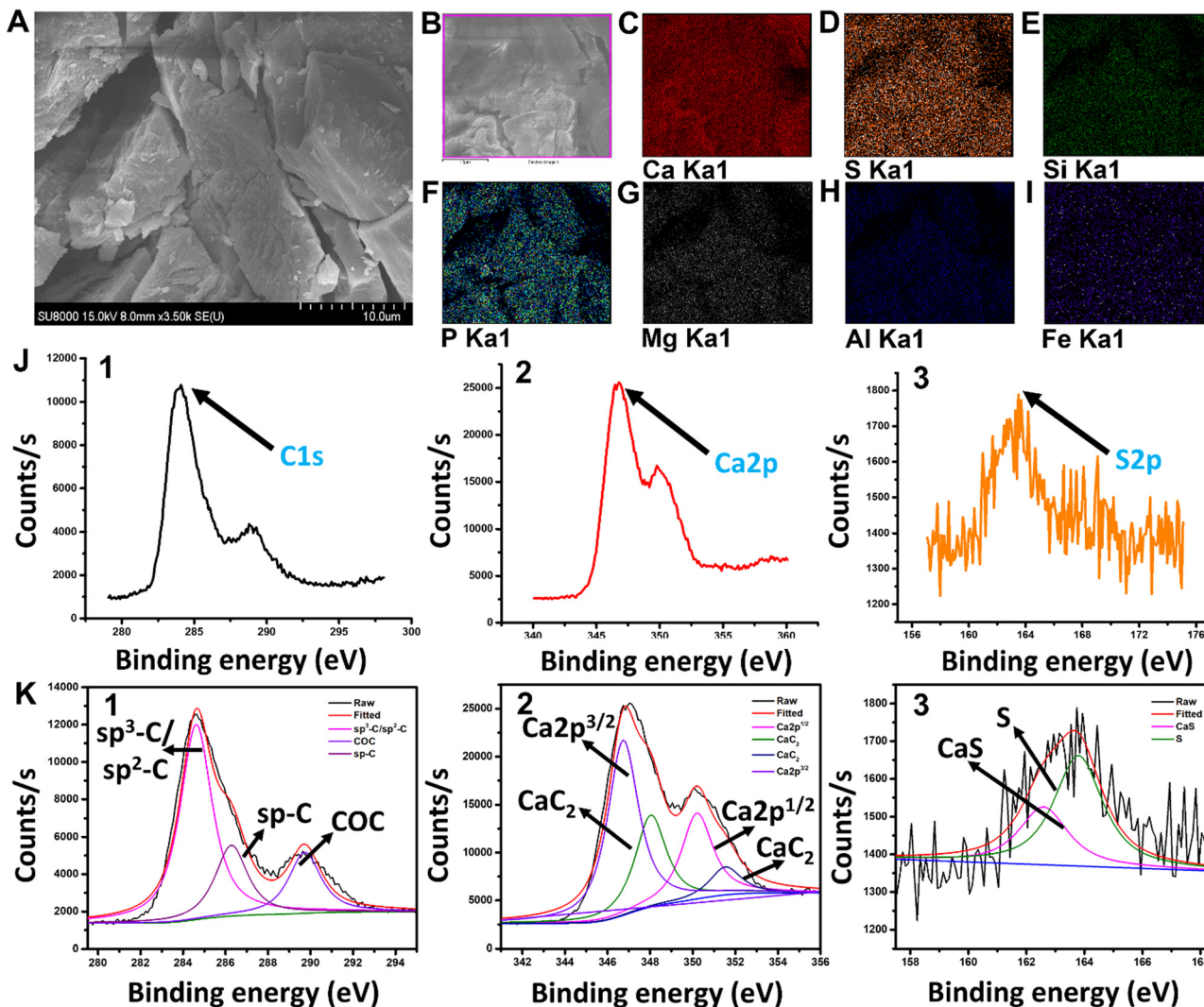


Fig. 1 (A) SEM image of CaC<sub>2</sub> at 10 μm. (B)–(I) Distribution of all elements and their core-level studies based on SEM mapping. (J1–J3) XPS data. (K1–K3) Fitted XPS data for carbon, calcium, and sulfur distribution.

### 3.2 DTNB solution as a CaC<sub>2</sub> sensor

DTNB is a chemical substance that is used to determine the concentration of free sulfhydryl groups in a sample. George L. Ellman came up with the concept and created this reagent by oxidizing 2-nitro-5-chlorobenzaldehyde to carboxylic acid, adding free sulfhydryl groups *via* sodium sulfide, and linking the monomer *via* iodine oxidation. CaS<sup>−</sup> free sulfhydryl groups of CaC<sub>2</sub> interact with this reagent, slicing the disulfide bond to form the TNB<sup>−</sup> anion,<sup>56</sup> which ionizes to TNB<sup>2−</sup> dianion in water at neutral and alkaline pH; TNB<sup>2−</sup> ions have a yellow color. One mole of free sulfhydryl groups releases one mole of TNB in this rapid and stoichiometric reaction. TNB<sup>2−</sup> was detected spectrophotometrically by measuring the visible light absorbance at 412 nm with an extinction coefficient of 14,150 M<sup>−1</sup> cm<sup>−1</sup> for dilute buffer solutions at pH 9.0 [Fig. 2(A)]. The DTNB buffer solution changed from colorless to yellow and then dark yellow after being exposed to CaC<sub>2</sub> [Fig. 2(E)].<sup>57</sup> CaC<sub>2</sub> is detected using DTNB because of its impurity form “CaS” contains a significant

amount of sulfide. This contaminant is produced during steel desulfurization in steel plants.<sup>4–6</sup>

When DTNB reacts with a free sulfhydryl group, mixed disulfide and TNB acid are formed [Fig. 2(F)]. DTNB targets the conjugate base (R-S<sup>−</sup>) “CaS<sup>−</sup>” of CaC<sub>2</sub>, the free sulfhydryl group in this reaction, producing TNB, a “colored” species with a high molar extinction coefficient in the visible region [Fig. 2(F)].<sup>58,59</sup> In the case of CaC<sub>2</sub>, the CaS<sup>−</sup> sulfide moiety (present as an impurity source from steel manufacturing industries) interacts with DTNB *via* the above stated mechanism. The standard linear curve fitting can be a good indicator of the assay's strength at 323 and 412 nm peaks [Fig. 2(C) and (D)]. To produce TNB and mixed disulfides, free sulfide groups interact stoichiometrically with TNB. Further at pH 9, TNB ionizes to TNB<sup>2−</sup> dianion in water. The color of TNB<sup>2−</sup> ions is yellow. Depending on the CaS concentration in CaC<sub>2</sub>, the color of the DTNB buffer solution changed from colorless to yellow and eventually to dark yellow after being exposed to CaC<sub>2</sub> [Fig. 2(F)]. As shown in Fig. 2(C), DTNB steadily reduces to TNB<sup>2−</sup> ions at low CaC<sub>2</sub> concentrations because there are less



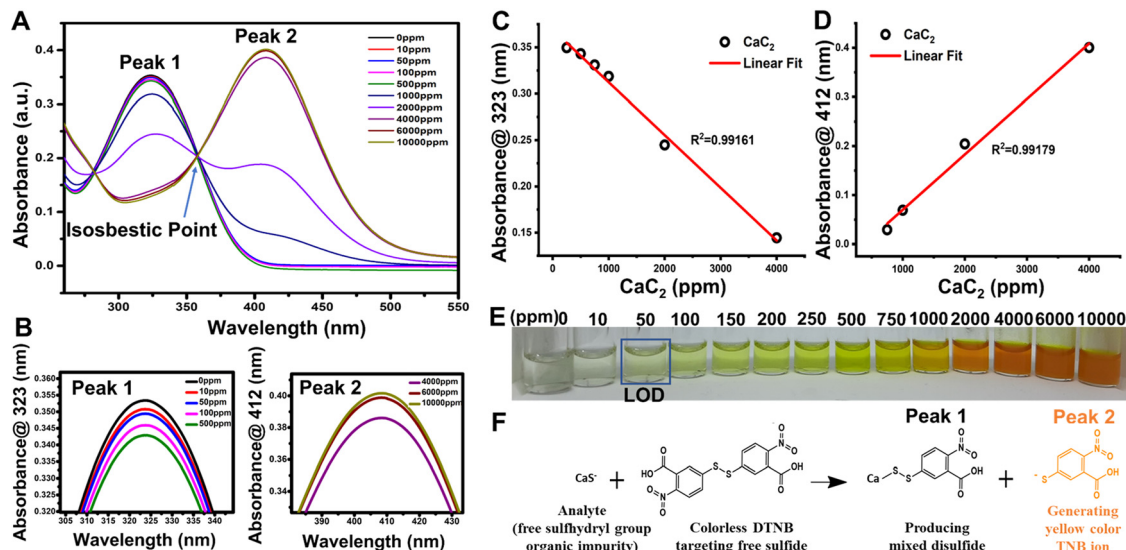


**Fig. 2** (A)  $\text{CaC}_2$  (0–10 000 ppm) detection absorbance spectra with a redshift in peaks from 323 to 412 nm, indicating the formation of TNB ions, which are responsible for the yellow color development. (B) Magnified representation of plot (A) for a clear understanding of absorption values at 323 and 412 nm peaks. (C) and (D) Linear curve fittings of the peaks at 323 and 412 nm, respectively, for standard  $\text{CaC}_2$  concentrations. (E) Solution based  $\text{CaC}_2$  colorimetric sensing, and (F) reduction of DTNB ions responsible for the redshift and color development.

sulfide ions available to interact with it. DTNB exhibits a spectroscopic absorbance peak at 323 nm, whereas  $\text{TNB}^{2-}$  exhibits a peak at 412 nm. All the DTNB undergoes a rapid stoichiometric reaction in the presence of high sulfide content and produces yellow color [Fig. 2(E)], as seen by the shift in the absorbance spectra of  $\text{TNB}^{2-}$ , which showed absorbance at a wavelength of 412 nm, instead of 323 nm as DTNB quickly converted to  $\text{TNB}^{2-}$  ions [Fig. 2(D)]. Ellman's assay has an isosbestic point of around 356 nm [Fig. 2(A)]. The isosbestic point can be determined either tabularly or graphically by measuring the full spectrum of the absorbance values for each solution to confirm that the molar ratio between Ellman's reagent and the test sample is equivalent across each test solution. A smooth peak at 412 nm also indicates that our solution is within the assay's working range. Fig. 2(C) and (D) depict the linear curve fittings of peaks at 323 and 412 nm, respectively, for standard  $\text{CaC}_2$  concentrations. Ellman's reagent can also be used to measure free sulfhydryl groups such as glutathione in pure solutions<sup>60</sup> as well as biological specimens such as blood.<sup>61</sup> It can also be used to determine the number of free sulfhydryl groups in proteins.<sup>62</sup> Despite the widespread use of Ellman's reagent in various sensing applications, no study has been published on using Ellman reagent-based sensors to detect  $\text{CaC}_2$  on fruit skin after  $\text{CaC}_2$  artificial ripening.

### 3.3. Quantification of sulfhydryl concentrations in an unknown sample

The absorbance spectra of unknown solutions can be compared to those of the standard curve to ensure that the concentrations of the solutions are within the standard curve's range [Fig. 3]. The absorbance values of unknown  $\text{CaC}_2$  samples 1, 2, 3, and 4 were plotted along the standard curve [Fig. 3(C) and (D)], and they corresponded to those of the standard curve.

The linear trend of the sensor for the unknown sample can be used to determine the amount of  $\text{CaC}_2$  present in banana peels [Fig. 3(C) and (D)]. The number of sulfhydryl groups in the unknown sample was quantified based on molar absorptivity. An 850  $\mu\text{L}$  aliquot of four different unknown samples mixed with 150  $\mu\text{L}$  of Ellman's reagent solution produced absorbances of (1) 0.294, (2) 0.463, (3) 0.326, and (4) 0.201 on using a 1 cm spectrophotometric cuvette, which was plotted linearly [Fig. 3(C) and (D)]. The sulfhydryl concentrations in ppm were calculated for the four different unknown samples a, b, c, and d, and the results corresponded to 5.72 ppm, 7.53 ppm, 3.6 ppm, and 4.73 ppm, respectively [Table S2, ESI<sup>†</sup>].

### 3.4. Selectivity and sensitivity of the DTNB solution as a $\text{CaC}_2$ sensor

The visual observation of color changes in association with UV absorbance spectra [Fig. 2(D)] supported the colorimetric change of DTNB to  $\text{TNB}^{2-}$  ions in the system in the presence of  $\text{CaC}_2$ . It was necessary to determine DTNB selectivity in response to other AFRAs. Thus, common ripening agents, such as ethephon, potassium sulfate, potassium dihydrogen orthophosphate, oxytocin, and ethylene glycol, were added to various vials containing the DTNB sensor solution and spectral analysis was carried out [Fig. 4(B)], and the results revealed that the DTNB sensor was only sensitive to  $\text{CaC}_2$ , with its color changing ability from colorless to yellow [Fig. 4(A)]. Additionally, by doing the assay five more times, we were able to test the reproducibility and sulfide content in five distinct batches of the same 500 ppm  $\text{CaC}_2$  concentration, as shown in [Fig. 4(C)]. Spectral analysis of all five batches confirmed that the sulfide content was similar. The response time of the DTNB sensor was measured by exposing the sensor to  $\text{CaC}_2$  solution and taking images at 1 min intervals. The sensor quickly changed color





Fig. 3 The performance of the DTNB sensor in  $\text{CaC}_2$  detection based on broad range concentration (0–10 000 ppm). (A) Absorbance spectra and ion formation, with a redshift in peaks from 323 to 412 nm for standard  $\text{CaC}_2$  concentrations, indicating the formation of TNB ions responsible for the yellow color development. (B) Absorption spectra of unknown samples 1, 2, 3, and 4, and (C) and (D) fitting of unknown sample concentrations in standard linear curves at peaks at 323 and 412 nm, respectively.

from colorless to yellow, and no further significant color change was observed after 10 min of exposure (negligible change) [Fig. 4(D)]. With the help of spectral analysis, it was confirmed that after 10 min, the formation of TNB ions got

saturated and no change in peak intensity was observed at concentrations of 50 and 100 ppm  $\text{CaC}_2$  [Fig. 4(E) and (F)]. In this study, time-dependent degradation of the colorimetric signal was performed, and it was discovered that the sensor's

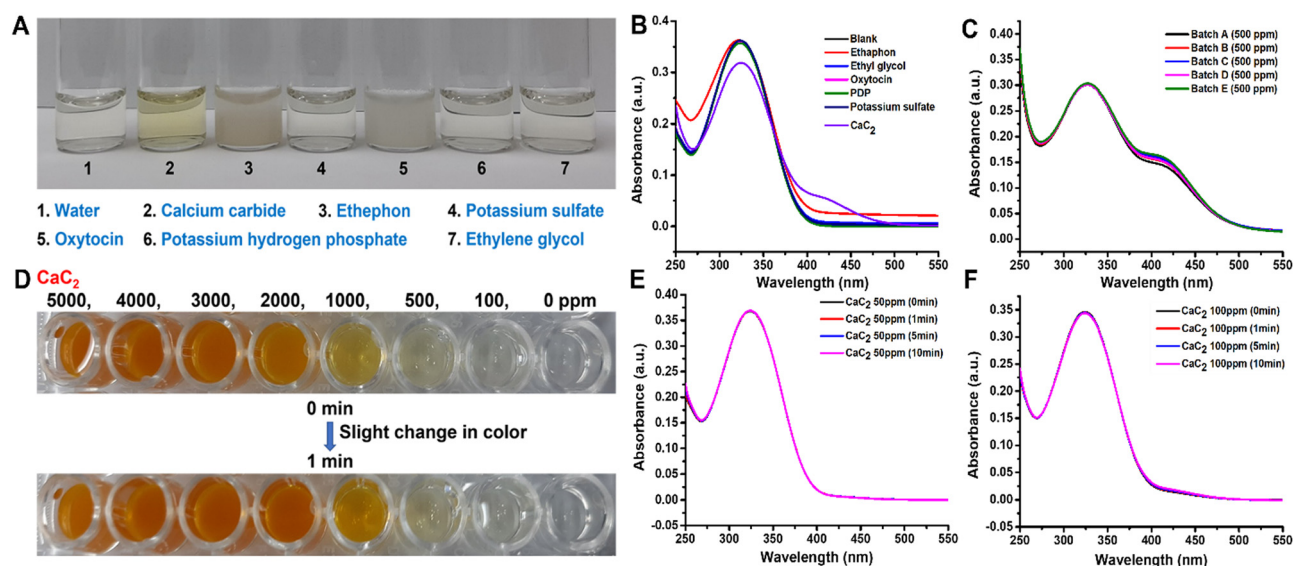


Fig. 4 DTNB sensor performance in the presence of other ripening agents as well as the time-dependent stability. (A) The DTNB sensor was exclusively sensitive to  $\text{CaC}_2$ , exhibiting a color change from colorless to yellow, and was insensitive to other less common ripening agents (ethaphon, potassium sulfate, potassium dihydrogen orthophosphate, oxytocin, and ethylene glycol) involved in the fruit-ripening process. (B) Spectral analysis of all interfering compounds. (C) Reproducibility and spectral analysis of  $\text{CaC}_2$  in different batches. (D) The sensor changed color quickly, and no further significant color change was observed after 1 min of exposure (negligible change). (E and F) Stability and time-dependent spectral analysis of 50 and 100 ppm  $\text{CaC}_2$ .



color remained stable for more than a month [Fig. S4, ESI†]. This rapid color change indicates that the free sulfide group from  $\text{CaC}_2$  reacted with the DTNB sensor to form TNB ions. The detection limit was calculated as the average value of absorbance at zero concentration with three standard deviations.<sup>63,64</sup> The DTNB sensors were exposed to different  $\text{CaC}_2$  concentrations ranging from 0 to 10 000 ppm, and their images were taken immediately to determine their limit of detection (LOD) for  $\text{CaC}_2$  [Fig. 2(E)]. When the  $\text{CaC}_2$  concentration was less than 50 ppm, the color change was quite visible to the naked eye. However, at concentrations of 100 ppm and above, the color change of the sensors was clearly visible. The LOD of the DTNB sensors corresponded to that of  $\text{CaC}_2$ .

### 3.5. Artificially ripened fruit monitoring

The developed DTNB-based sensor was used for real-time monitoring of  $\text{CaC}_2$  in banana fruit peels as a model sample for our work in order to demonstrate its practical application for  $\text{CaC}_2$  monitoring. Our sensor is applicable to other fruits as well, such as mango, pear, apple, papaya, grapes, plum, *etc.*, which are considered for the artificial ripening treatment. The color transitioning pattern of the banana-exposed sensor [Fig. 5] was found to be similar to that of the pure  $\text{CaC}_2$ -exposed sensor.

### 3.6. Monitoring of the matrix effect and other sulfates

We used the proposed sensor to test the interference of the natural sulfate content and the additional sulfate contents in the banana matrix. It was discovered that there was no interference effect of matrix and other sulfates (ammonium sulfate, manganese sulfate, magnesium sulfate, potassium sulfate, sodium sulfate, and copper sulfate) [Fig. S2 and S5, ESI† respectively]. According to the one-step analysis, our proposed sensor demonstrated the best performance for  $\text{CaC}_2$  detection with high sensitivity and selectivity immediately after being exposed to samples.

### 3.7. Assessment of sensor performance

Currently, colorimetric sensors are very attractive due to their inherent advantages of direct understanding of detection results, portability, low-cost efficiency, user-friendliness, and high sensitivity. Only one colorimetric assay has been published for  $\text{CaC}_2$  detection; however, it does not meet the basic requirements as it is complicated and non-portable, and requires a trained person for handling. To combat such challenges, we proposed a simple sensor and the performance of our  $\text{CaC}_2$  sensor is compared with other prominent work in Table 1. For all existing techniques complicated methods, difficulty in understanding at the consumer level, and non-



Fig. 5 (1–6)  $\text{CaC}_2$  monitoring using the DTNB sensor on the skin of artificially ripened bananas, with a step-by-step illustration of real-time sensing.



Table 1 Comparison of the fabricated CaC<sub>2</sub> sensor performance with those of the existing ones

Sensing technology	Fruit	Analyte	LOD	Time	Handling	Portable	Ref.
Infrared thermal emission sensor	Banana	Ethylene	5 ppm	—	Complicated	No	65
LS-capped AuNP sensor	Mango	CaC <sub>2</sub>	0.01 ppm	5 min	Complicated	No	40
HPLC/MS/MS	Banana	Ethephon	0.92 ppm	—	Complicated	No	66
Image processing/multispectral imaging sensor	Banana	—	—	—	Complicated	No	67
DTNB colorimetric sensor	Banana	CaC <sub>2</sub>	50 ppm	Prompt	Simple and user friendly	Yes	Present work

portability are the main concerns to be solved. Due to complex methodologies, these methods are expensive and instrument dependent as well as require expensive chemicals. Our sensor has simplified the assay method and results are understandable by applying one step detection. As summarized in Table S3 (ESI<sup>†</sup>), the presented sensor enhanced the sensitivity and selectivity, reduced sensing time and sample volume, also it is very convenient and portable when compared to other existing techniques as it is just a small bottle containing our active sensing solution and consumers just need to add few drops of sample to the test bottle. Overcoming all concerns and fulfilling all needs, creating our sensor could be a potentially ASSURED tool for CaC<sub>2</sub> detection in ARFs and filling the gap between laboratory-based analysis and on-site detection of analytes for a variety of purposes. The developed sensor must meet a few important specifications for its validation; it is all about sensor resolution, accuracy, and precision. The relative standard deviation (RSD) of the developed sensing in response to 50 ppm CaC<sub>2</sub> for ten measurements was observed as less than 5.0%, indicating good reproducibility of the developed sensor. The shelf life of the developed sensing solutions and their sensing responses were checked every two days for two weeks with 50 ppm CaC<sub>2</sub>. The sensing solutions were stored at refrigerator temperature to monitor the storage stability. Each experiment was performed in triplicate. After two weeks of storage, the developed sensing solution retained about 92.5% of its initial response, indicating good storage stability and precision preferences.

### 3.8. Comparative study and validation of the DTNB-based sensor

A comparative study is required for the validation and assessment of the developed method against other credible traditional methods for ARF monitoring assurance. We performed and compared the CaC<sub>2</sub> analysis using our developed method and ICP-OES to confirm the presence of sulfide content and the linearity, sensitivity, and accuracy of our developed method for its validation. Fig. S6 (ESI<sup>†</sup>) depicts the ICP-OES's and our sensor's comparative absorbance linear plot of sulfide content in standard CaC<sub>2</sub> solutions with *R*<sup>2</sup> of 0.9895 and 0.9732, respectively. Data comparison demonstrates our sensor's linearity and sensitivity. Table S3 (ESI<sup>†</sup>) compares the detection patterns of sulfide in CaC<sub>2</sub> using the developed sensor (visual/colorimetric data for naked eye readability in the CaC<sub>2</sub> sample) and the detection analyzed using the traditional technique (ICP-ES data for sulfide quantification in the CaC<sub>2</sub> sample). It has been observed that the developed method has the ability to show instant color change-based detection at the CaC<sub>2</sub> concentration of 50 ppm; however, in ICP-MS, the detection

is based on total detectable sulfide content *via* an analytical technique which may also show recovery losses in trace sulfide content analysis. In addition to this, the complete analytical procedure of ICP-MS requires several typical steps, such as sample extraction (2–3 h), and a single sample run of 20–30 min for sulfide content detection in CaC<sub>2</sub>, which could be eliminated *via* the currently developed detection method.

## 4. Conclusions

A colorimetric CaC<sub>2</sub> sensor was developed using an optimized enzymatic receptor DTNB solution. This paper describes the sensing and characterization of CaC<sub>2</sub> using an enzymatic chemoreceptor. The sensor was discovered to significantly detect the presence of CaC<sub>2</sub> in banana fruit peels. Our results revealed that the DTNB reagent emits a colorimetric (yellow) signal when it comes into contact with CaC<sub>2</sub>. This signal indicates the presence of sulfide in CaC<sub>2</sub>. The DTNB sensor is simple, and it responds to artificially ripened fruits, such as bananas, by exhibiting a strong color change from colorless to yellow to dark yellow. The sensor only responds to CaC<sub>2</sub> when exposed to another ripening agent. Furthermore, this work was optimized to prevent the consumption of artificially ripened fruits. The color transition of the DTNB enzymatic chemoreceptor sensors was discovered to have a linear relationship with increasing CaC<sub>2</sub> levels, and a redshift was observed after reaching the isosbestic point. Based on this linear trend, the LOD using a UV spectrophotometer was 10 ppm, while the LOD with the naked eye was 50 ppm.

## Author contributions

Sonam Sonwal: writing – original draft, investigation, methodology, validation, and data curation. Shruti Shukla: data curation and writing – review and editing. Munirah Alhammadi: writing – review and editing. Reddicherla Umapathi: writing – review and editing. Hemanth P. K. Sudhani: writing – review and editing. Youngjin Cho and Yun Suk Huh: conceptualization, funding acquisition, writing – review and editing, and supervision.

## Conflicts of interest

The authors declare no conflict of interest.

## Acknowledgements

This research was supported by the Main Research Program (E0211002-03) of the Korea Food Research Institute (KFRI) funded



by the Ministry of Science and ICT. Authors are also thankful for the Department of Biotechnology-Ramalingaswamy fellowship, India research grant (BT/RLF/Re-entry/20/2017, awarded to Shruti Shukla) for completing this study.

## References

- M. Nag, B. Nag, S. Gangopadhyay, P. Panigrahi and B. Singh, *Eng. Failure Anal.*, 2021, **125**, 105384.
- F. N. H. Schrama, E. M. Beunder, S. K. Panda, H. J. Visser, E. Moosavi-Khoonsari, J. Sietsma, R. Boom and Y. Yang, *Ironmaking Steelmaking*, 2021, **48**, 1–13.
- M. Transparency, Report on: Calcium Carbide Market, Report number:TMRGL42740, USA, 2021.
- F. N. H. Schrama, E. M. Beunder, S. K. Panda, H. J. Visser, E. Moosavi-Khoonsari, J. Sietsma, R. Boom and Y. Yang, *Ironmaking Steelmaking*, 2021, **48**, 1–13.
- W. E. Caldwell and F. C. Krauskopf, *J. Am. Chem. Soc.*, 1929, **51**, 2936–2942.
- D. Lindstrom, S. Karamoutsos and S. Du, *Book on: Study on desulphurization of hot metal using different agents*, 2015.
- M. Roy, S. Langthasa and D. N. Hazarika, *J. Pharmacogn. Phytochem.*, 2021, **10**, 432–436.
- A. Abdul, M. Qadir, F. Sardar, R. Sobia, F. Rahman and M. Ghulam, Book on: Biotechnological Strategies for Promoting Invigorating Environs, *Phytoremediation*, 2022.
- B. Mahajan, Report on: How safe are our fruits? Chemical ripening is assuming endemic proportions, *The Tribune (Voice, of the People)*, 2018.
- T. Wilson, Report on: Artificially ripened fruits find place on racks despite crackdown, *THE HINDU*, Coimbatore, India, 2019.
- K. N. Chaturvedi, Report on: Food Law; Food Safety and Standard ACT, 2006, *Food Safety and Standards Authority of India*, 2023.
- A. Panghal, D. N. Yadav, B. S. Khatkar, H. Sharma, V. Kumar and N. Chhikara, *Nutr. Food Sci.*, 2018, **48**(4), 561–578.
- K. Pannu, Report on: Watch out for artificial ripeners, *The Tribune (Voice, of the People)*, 2019.
- M. V. Ambwani, Report on: Agri Business; FSSAI to clamp down on artificial ripening of fruits using banned substances, New Delhi, 2019.
- A. Maindola, Report on: FSSAI to inspect & monitor fruits & vegetables for calcium carbide use, New Delhi, 2019.
- FSSAI, Asian Age, 2019, p. 1.
- FSSAI, Sentin. this land, its people, 2019, p. 1.
- FSSAI, Ntooz my city my newz, 2018, p. 2.
- B. P. Deepu, *New Indian Express*, 2018, 3.
- A. M. Ekanem, W. N. Sylvanus, Q. E. Asanana, I.-O. I. Akpabio, E. I. Clement, C. K. Okpara, B. E. Okon and K. E. George, *J. Adv. Med. Med. Res.*, 2021, **33**, 72–83.
- R. Sharma, M. A. Coniglio and L. Pasqualina, *Fruits and Vegetables, Though Rich in Antioxidants, Might Lead to Cytotoxicity*, Springer, Cham, 2022.
- R. Sharma, M. A. Coniglio and L. Pasqualina, *Determination of Inflammatory Molecules in Fruits and Vegetables*, Springer, Cham, p. 2021.
- D. Candra, D. Mahmudy, W. Firdaus, W. Arisoelaningsih, S. Endang and S. Solimun, *Review of Non-Destructive Banana Ripeness Identification using Imagery Data, Association for Computing Machinery*, New York, NY, USA, 2021.
- A. T. Lacap, E. R. V. Bayogan, L. B. Secretaria, M. I. A. Tac-an and C. D. S. Lubaton, *Mindanao J. Sci. Technol.*, 2021, **19**, 40–58.
- FSSAI, Hindu, Press Trust, India, 2020, p. 2.
- S. Kannappan, J. Chang, P. R. Sundharbaabu, J. H. Heo, W. Kee Sung, J. C. Ro, K. K. Kim, J. B. B. Rayappan and J. H. Lee, *Biochip J.*, 2022, **16**, 490–500.
- H. H. Cho, J. H. Heo, D. H. Jung, S. H. Kim, S. J. Suh, K. H. Han and J. H. Lee, *Biochip J.*, 2021, **15**, 276–286.
- C. H. Cho, T. J. Park and J. P. Park, *Biotechnol. Bioprocess Eng.*, 2022, **27**, 607–614.
- A. Ravindran, R. Anitha and A. Ravindran, *Int. J. Eng. Res. Sci. Technol.*, 2015, **4**, 791–794.
- R. Umapathi, S. Sonwal, M. J. Lee, G. Mohana Rani, E. S. Lee, T. J. Jeon, S. M. Kang, M. H. Oh and Y. S. Huh, *Coord. Chem. Rev.*, 2021, **446**, 214061.
- R. Umapathi, B. Park, S. Sonwal, G. M. Rani, Y. Cho and Y. S. Huh, *Trends Food Sci. Technol.*, 2022, **119**, 69–89.
- R. Umapathi, S. M. Ghoreishian, S. Sonwal, G. M. Rani and Y. S. Huh, *Coord. Chem. Rev.*, 2022, **453**, 214305.
- R. Singh, N. Kumar, R. Mehra, H. Kumar and V. P. Singh, *Trends Environ. Anal. Chem.*, 2020, **26**, e00086.
- P. Chawla, R. Kaushik, V. J. Shiva Swaraj and N. Kumar, *Environ. Nanotechnol., Monit. Manage.*, 2018, **10**, 292–307.
- H. Patel, D. Rawtani and Y. K. Agrawal, *Trends Food Sci. Technol.*, 2019, **85**, 78–91.
- A. Pankaew, J. Rueangsuwan, R. Traiphol and N. Traiphol, *J. Ind. Eng. Chem.*, 2022, **111**, 519–529.
- R. Saymung, A. Watthanaphanit, N. Saito, N. Traiphol and R. Traiphol, *J. Ind. Eng. Chem.*, 2022, **106**, 243–252.
- K. J. Land, D. I. Boeras, X. S. Chen, A. R. Ramsay and R. W. Peeling, *Nat. Microbiol.*, 2019, **4**, 46–54.
- M. S. Khan, S. A. Shadman and M. M. R. Khandaker, *Curr. Opin. Chem. Eng.*, 2022, **35**, 100733.
- A. J. Lakade, K. Sundar and P. H. Shetty, *Food Addit. Contam., Part A: Chem., Anal., Control, Exposure Risk Assess.*, 2018, **35**, 1078–1084.
- I. Raya, H. H. Kzar, Z. H. Mahmoud, A. Al Ayub Ahmed, A. Z. Ibatova and E. Kianfar, *Carbon Lett.*, 2022, **32**, 339–364.
- Y. Yi, B. Wang, X. Liu and C. Li, *Carbon Lett.*, 2022, **32**, 713–726.
- M. J. Deka, D. Chowdhury and B. K. Nath, *Carbon Lett.*, 2022, **32**, 1131–1149.
- R. T. Yogeeshwari, R. H. Krishna, P. S. Adarakatti and S. Ashoka, *Carbon Lett.*, 2022, **32**, 181–191.
- P. Rawat, P. Nain, S. Sharma, P. K. Sharma, V. Malik, S. Majumder, V. P. Verma, V. Rawat and J. S. Rhyee, *Luminescence*, 2022, 1–22.
- P. Rawat, P. Kumar Sharma, V. Malik, R. Umapathi, N. Kaushik and J. S. Rhyee, *Mater. Lett.*, 2022, **308**, 131241.
- P. Kumar Sharma, A. Ruotolo, R. Khan, Y. K. Mishra, N. Kumar Kaushik, N. Y. Kim and A. Kumar Kaushik, *Mater. Lett.*, 2022, **308**, 131089.



- 48 P. K. Sharma, E. S. Kim, S. Mishra, E. Ganbold, R. S. Seong, A. K. Kaushik and N. Y. Kim, Ultrasensitive and reusable graphene oxide-modified double-interdigitated capacitive (DIDC) sensing chip for detecting SARS-CoV-2, *ACS Sens.*, 2021, **6**(9), 3468–3476, DOI: [10.1021/acssensors.1c01437](https://doi.org/10.1021/acssensors.1c01437).
- 49 W. M. N. H. W. Salleh, N. M. Shakri, M. A. Nafiah and S. Khamis, *Lat. Am. Appl. Res.*, 2022, **52**, 73–76.
- 50 J. Zamanian, Z. Khoshbin, K. Abnous, S. M. Taghdisi, H. Hosseinzadeh and N. M. Danesh, *Biosens. Bioelectron.*, 2022, **197**, 113789.
- 51 H. Lawal, Report on: Concern as carbide-ripened fruits flood Abuja, Nassarawa markets, *Enviro News*, 2017.
- 52 J. Yang, Y. Chen, J. Peng, J. Zeng, G. Li, B. Chang, Y. Shen, X. Guo, G. Chen, X. Wang and L. Zheng, *J. Energy Storage*, 2022, **51**, 104473.
- 53 Y. Jia, X. Chen, G. Zhang, L. Wang, C. Hu and X. Sun, *J. Mater. Chem. A*, 2018, **6**, 23638–23643.
- 54 A. Al-Mamoori, S. Lawson, A. A. Rownaghi and F. Rezaei, *Energy Fuels*, 2019, **33**, 1404–1413.
- 55 S. Murugan, S. Niesen, J. Kappler, K. Küster, U. Starke and M. R. Buchmeiser, *Batteries Supercaps*, 2021, **4**, 1636–1646.
- 56 P. Suwannapattana, M. Kongkaew, W. Thongchai and N. Sirasunthorn, *Chem. Biodiversity*, 2023, **20**(7), 1612–1872, DOI: [10.1002/cbdv.202300171](https://doi.org/10.1002/cbdv.202300171).
- 57 A. F. Boyne and G. L. Ellman, *Anal. Biochem.*, 1972, **46**, 639–653.
- 58 H. Zhou, PhD thesis, Georgia State University, 2019.
- 59 K. M. Schaich, *Book on: Analysis of Lipid and Protein Oxidation in Fats, Oils, and Foods*, AOCS Press, 2016, pp. 1–131.
- 60 J. O. Olugbodi, B. Lawal, G. Bako, A. S. Onikanni, S. M. Abolenin, S. S. Mohammad, F. S. Ataya and G. E. Batiha, *Sci. Rep.*, 2023, **13**, 10539.
- 61 S. R. Mendes, F. X. Gomis-Rüth and T. Goulas, *Sci. Rep.*, 2023, **13**, 1–9.
- 62 H. Y. Lai, M. I. Setyawati, C. V. Duarte, H. M. Chua, C. T. Low and K. W. Ng, *J. Biomed. Mater. Res., Part B*, 2023, **111**, 933–945.
- 63 S. Park, S. Shukla, Y. Kim, S. Oh, S. Hun Kim and M. Kim, *Microbiol. Immunol.*, 2012, **56**, 472–479.
- 64 S. Shukla, Y. Haldorai, I. Khan, S. M. Kang, C. H. Kwak, S. Gandhi, V. K. Bajpai, Y. S. Huh and Y. K. Han, *Mater. Sci. Eng., C*, 2020, **113**, 110916.
- 65 J. Kathirvelan and R. Vijayaraghavan, *Infrared Phys. Technol.*, 2017, **85**, 403–409.
- 66 P. K. Phuong, L. T. Hoa, L. M. Q. Cuong and L. Duan, *Int. J. Food Sci. Agric.*, 2021, **5**, 26–32.
- 67 V. Hallur, B. Atharga, A. Hosur, B. Binjawadagi and K. Bhat, *Proc. Int. Conf. Circuits, Commun. Control Comput. I4C 2014*, vol. 2014, pp. 139–140.

